

# Chapter 9

## Spatial and Temporal Order Beyond the Deterministic Limit: The Role of Stochastic Fluctuations in Population Dynamics

Duccio Fanelli

**Abstract** Modeling the self-consistent dynamics of an ensemble made of microscopic constituents can be tackled via deterministic or alternatively stochastic viewpoints. The latter enables one to respect the discrete nature of the scrutinized medium, a possibility which is conversely prevented when dealing with the former idealized approximation. As we shall here discuss, stochastic finite-size fluctuations can drive the emergence of regular spatiotemporal cycles that persist for moderate and even large sizes of the population and which are not captured within the mean-field descriptive scenario. The van Kampen system-size expansion is an elegant mathematical approach that allows one to investigate the key role played by the inherent stochasticity. We here provide a pedagogical introduction to such a method and discuss its application to a model of autocatalytic reactions.

### 9.1 Introduction

Investigating the dynamical evolution of microscopic entities in mutual interaction constitutes a rich and fascinating problem of paramount importance and cross-disciplinary interest [1]. Molecules, with their chemical properties and distinct diffusive abilities, can be ideally grouped into homogeneous families, whose concentrations vary continuously with position and time, as follows the governing dynamics [2, 3]. Similarly, families of organisms (animals, plants) can be identified in any ecological system, competition, and cooperation driving their interlaced evolution [1, 4]. Analogous concepts translate to the realm of social science

---

D. Fanelli (✉)

Dipartimento di Energetica, University of Florence, via S. Marta 3 50139, Florence, Italy

Dipartimento di Fisica e Astronomia, University of Florence,

via Sansone 1 50019 Sesto Fiorentino, Florence, Italy

e-mail: [duccio.fanelli@unifi.it](mailto:duccio.fanelli@unifi.it)

applications and human communities models. In general terms, and irrespectively of the specific context of investigation, it is customary to refer to a population as to a macroscopic, extended group composition of a large sea of homologous microscopic actors. From biology to biomedicine, passing through physics and chemistry, the study of population dynamics is often tackled via a simplistic approach: the scrutinized families are assumed to be composed of an infinite collection of constitutive elements. Correlations are then neglected so to favor a mean-field description, which in many cases enables for straightforward analytical progress. The system is hence treated in the continuum limit and the interactions link the families as a whole. However, single individual effects, stemming from the intimate discreteness of the analyzed medium, can prove crucial by modifying significantly the mean-field predictions and so opening up the perspective for alternative explanations of a wide gallery of experimental observations [5, 6]. It has been shown in fact that the stochastic component of the microscopic dynamics, resulting from the aforementioned discreteness and thus associated to finite-size corrections, can induce regular macroscopic patterns, both in time and space [7–13]. The effect of the graininess materializes in an endogenous source of disturbance, also termed demographic noise, opposed to other perturbations that can be imagined to persist in the continuum limit. The fact that the demographic noise, intrinsic to the system, can spontaneously drive the emergence of regular structures, reflecting a degree of temporal and spatial macroscopic order, is in some respect counterintuitive and intriguing per se. In this chapter we shall provide an introductory description to population dynamics, highlighting the different approaches, as outlined above. We will in particular discuss a simple birth/death process, making explicit the distinct philosophies that inspire the deterministic and stochastic paradigms, and introduce the relevant mathematical concepts. Then we will move forward by reviewing a specific case study, for which both temporal and spatial order manifests, as mediated by the microscopic stochastic component of the dynamics.

## 9.2 On the Deterministic and Stochastic Viewpoints

The study of the dynamical evolution of interacting species of homologous quantities defines the field of population dynamics [1, 14], which, as previously emphasized, finds particularly relevant applications in life science [2, 3]. Population is indeed a technical wording which encompasses distinct fields of investigations ranging from, e.g., the level of expression of a protein in a cell to the number of animals in a finite ecosystem [1, 4]. The classical approach to population dynamics relies on characterizing quantitatively the densities of species through a system of ordinary differential equations which incorporates for the specific interactions being at play. Pure competition, predator-prey interactions, or even cooperative effects could be translated into dedicated interaction terms [1, 4] via a straightforward application of the law of mass action. Specific delays might be required to account

for the processing time which is often necessary to react to an external stimulus or signal, a paradigmatic problem of many biological pathways. More than one independent variable is often to be assumed, which in turn implies dealing with systems of partial differential equations. As an example, when tracing the dispersion of a diffusing chemical compound, space and time are to be explicitly represented into the mathematical description. All these phenomena can be tackled via the population viewpoint by focusing on the mutual evolution of the families in which the elementary constituents are ideally grouped. It is customary to refer to this level of description as to the *deterministic theory*. Noise and other disturbances can be eventually hypothesized to alter the ideal deterministic, hence reproducible, dynamics but always act as a macroscopic bias.

As opposed to this formulation, a different level of modeling can be invoked focusing instead on the *individual-based description* [5, 6] which is intrinsically *stochastic*. This amounts to characterizing the microscopic dynamics via transition probabilities governing the interactions among individuals and with the surrounding environment. This approach has been recently adopted in various contexts such as predator-prey interactions, metabolic reactions, and epidemic models. The stochasticity of the systems stems from the microscopic finiteness/discreteness of the dynamical variables involved.

Deterministic and stochastic pictures, conceptually alternative, yield to different descriptions of a scrutinized phenomenon. It is therefore of interest to highlight similarities, and/or discrepancies, in the associated predictions. A viable method that enables one to bridge the gap between the deterministic and stochastic scenarios is the celebrated van Kampen's system-size expansion [6]. The idea goes as follows. Start from a stochastic, individual-based model, which formally corresponds to dealing with a master equation for the probability of photographing the system in a given configuration at a specific time. Then, perform a perturbative expansion with respect to a small parameter which encodes for the amplitude of fluctuations, or in other terms, the finite size of the system (e.g., total number of molecules or organisms). At the leading order of the perturbative calculation one recovers the mean-field equations, namely, the deterministic description alluded above. Including the next-to-leading order corrections, one obtains a description of the fluctuations, as a set of linear stochastic differential equations. Such a system can be analyzed exactly, so allowing one to quantify the differences between the stochastic formulation and its deterministic analogue. Let us emphasize again that fluctuations do not arise from an externally imposed noise source. It is the intimate discreteness of the system which results in an unavoidable intrinsic noise, a key contribution to the dynamics that has to be considered in any sensible model of natural phenomena, where a finite, though large, number of actors are simultaneously at play. These are important aspects, often omitted in the literature, and, due to their common origin, bear intriguing traits of universality across various disciplinary fields. Importantly, the inner stochastic component, also termed demographic noise, can yield to regular spatiotemporal patterns [7–13], signaling a degree of cooperativity and collective organization which instead lacks in the corresponding mean-field description.

The fact that fluctuations can be enhanced by a resonant effect was conjectured by Bartlett [15] in the context of the modeling of measles epidemics and later elaborated upon by Nisbet and Gurney [16], who called these stochastically induced oscillations, quasi-cycles. However, it is only in the last few years that these effects have been explained in rigorous terms, yielding to quantitative understanding of the phenomenon [7]. In the following, we shall elaborate on these important, and rather general, facts by selecting one specific case study. This is a scheme of autocatalytic reaction thoroughly studied in [11, 12]. The analysis presented in [11, 12] will be reviewed all along this chapter. Before that, next section is devoted to introducing the concept of master equation and to briefly discussing the van Kampen expansion technique.

### 9.3 The Van Kampen Expansion Applied to a Simple Birth/Death Stochastic Model

Consider a microscopic element  $X$ , which belongs to a given population, hereafter referred to as a species. Such an element can eventually die, leaving behind an empty space, called  $E$ . This simple event is exemplified by the following chemical equation:



where  $d$  is the reaction rate for a death to occur. Similarly, the spontaneous production of an individual element of type  $X$  is ruled by the chemical reaction



where  $b$  stands for the birth reaction rate. Further, let us assume that the number of microscopic entities, including the empties, totals in  $N$ , at time  $t = 0$ .  $N$  is clearly a conserved quantity of the dynamics if the system is forced to obey to the above chemical rules: every time one element of type  $X$  (resp.  $E$ ) disappears, it gets immediately replaced by one element  $E$  (resp.  $X$ ), so keeping the global population, sum of all individuals  $X$  and  $E$ , unchanged. Let us call  $n$  the number elements of type  $X$  and  $n_E$  the number of vacancies. Hence,  $n_E = N - n$  and the system is fully specified once the integer  $n$  is being assigned.

The process that obeys to chemical equations (9.1) and (9.2) is stochastic. Mathematically, it can be described in terms of a master equation that governs the evolution of the probability  $P(n, t)$  of seeing the system in a given configuration  $n$  at time  $t$ . To write such an equation one needs to quantify the transition rates  $T(n'|n)$  from an initial state  $n$  to a final one, labeled with  $n'$  and compatible with the former.

The transition rate associated to, e.g. the chemical equation (9.1) can be readily evaluated as the product of (i) the probability  $P_1$  of selecting one element of type  $X$  with (ii) the reaction constant  $d$ , which ultimately quantifies the probability that the selected individual eventually dies. Assume the individual entities, both the empties

and the material elements  $X$ , to be uniformly distributed inside the volume that hosts the system. Then,  $P_1 = n/N$  and this immediately yields to

$$T(n-1|n) = d \frac{n}{N} \quad (9.3)$$

Similarly, the transition rate associated to reaction (9.2) can be evaluated as

$$T(n+1|n) = b \frac{n_E}{N} = b \left(1 - \frac{n}{N}\right)$$

Under the above assumptions the system is Markov and the master equation for the probability  $P(n, t)$  reads

$$\begin{aligned} \frac{dP(n, t)}{dt} = & -T(n-1|n)P(n, t) + T(n|n+1)P(n+1, t) \\ & -T(n+1|n)P(n, t) + T(n|n-1)P(n-1, t) \end{aligned} \quad (9.4)$$

This equation provides a self-consistent and fully rigorous representation of the stochastic model defined by chemical Eqs. (9.1) and (9.2).

Starting from this setting, one can extract information on the average behavior of the system by neglecting the finite-size fluctuations and focusing on the time evolution of the mean-field concentration  $\langle n \rangle$  defined as

$$\langle n \rangle = \sum_n n P(n, t)$$

To this end, multiply by  $n$  both sides of Eq. (9.4) and sum over all possible states. The left-hand side takes the form

$$\sum_n n \frac{dP(n, t)}{dt} = \frac{d}{d(t/N)} \sum_n \frac{n}{N} P(n, t) = \frac{d\langle n \rangle}{d\tau} \quad (9.5)$$

where  $\tau = t/N$ . Focus now on the right hand side of Eq. (9.4), modified by the multiplicative factor  $n$ . Consider the first two terms:

$$\sum_n n [T(n|n+1)P(n+1, t) - T(n-1|n)P(n, t)] \quad (9.6)$$

$$= \sum_{n'} (n' - 1) T(n' - 1|n') P(n', t) - \sum_n n T(n-1|n) P(n, t) \quad (9.7)$$

$$= - \sum_{n'} T(n' - 1|n') P(n', t)$$

Changing  $n'$  into  $n$  and recalling the definition of  $T(n-1|n)$  one eventually obtains

$$- \sum_n d \frac{n}{N} P(n, t) = -d \frac{\langle n \rangle}{N} \quad (9.8)$$

Proceeding in a similar way, the last two terms in the right-hand side of the modified master equation yield to

$$b \left( 1 - \frac{\langle n \rangle}{N} \right) \quad (9.9)$$

Introduce now  $\phi = \langle n \rangle / N$ . Then collecting together the above contributions one eventually gets

$$\frac{d\phi}{d\tau} = b - (b + d)\phi. \quad (9.10)$$

The above ordinary differential equation governs the evolution of the continuum concentration  $\phi$ . The fluctuations have been in fact dropped out by performing the ensemble average  $\langle \cdot \rangle$ . Equation (9.10) can be solved analytically to yield

$$\phi(\tau) = \frac{b}{d+b} \left[ 1 - \left( 1 - \phi_0 \frac{b+d}{b} \right) \exp[-(b+d)\tau] \right] \quad (9.11)$$

Asymptotically the system converges to a stable fixed point,  $\phi^* = \frac{b}{d+b}$ . The above solution constitutes an ideal representation of the exact dynamics (9.4). Finite-size corrections materialize in fact in stochastic fluctuations that can sensibly affect the observed dynamics. To bring into evidence such an important aspect one can perform stochastic simulations of the chemical scheme (9.1) and (9.2) by means of the celebrated Gillespie algorithm [17, 18]. Such an algorithm produces realizations of the stochastic dynamics which are equivalent to those obtained from the governing master Eq. (9.4). In Fig. 9.1 the result of the stochastic simulations (wiggling line, black online) is compared to the deterministic solution (9.10) (smooth line, red online). The stochastic, hence exact, dynamics follows closely the idealized profile predicted by the mean-field theory. Fluctuations are however present and reflect the probabilistic nature of the problem in its original formulation. The statistics of the disturbances is investigated in Fig. 9.2 where the histograms of the quantities  $n/N - \phi$ , as recorded in direct Gillespie-based simulations, are plotted for different choices of the total population amount  $N$ . The profiles are Gaussian, as revealed by visual inspection. Importantly, the width of the distributions shrinks as  $1/\sqrt{N}$ . Hence, the fluctuations virtually disappear in the limit of infinite system size  $N \rightarrow \infty$  and consequently  $\phi \equiv \lim_{N \rightarrow \infty} n/N$ .

Fluctuations prove however crucial for any physical system made of a finite, though large, number of constitutive elements. Equations such as (9.4) are nonetheless difficult to analyze, and one has to rely on approximate techniques to elaborate on the role of stochasticity. The famous system-size expansion, pioneered by van Kampen [6] in the sixties, provides an elegant way of capturing the essential aspects of the discrete model, thus enabling one to appreciate the contribution of demographic, finite  $N$ , fluctuations. In the following and with reference to the simple birth/death process here considered, we will discuss the main assumptions of the method as well as its formal application. As a final result, we will be able to predict the distribution of the fluctuations, as seen in numerical simulations.

**Fig. 9.1** Temporal evolution of the species concentrations. The wiggling line refers to the stochastic simulations,  $n/N$  vs. rescaled time  $\tau$ . The smooth profile is the deterministic solution,  $\phi(\tau)$ . (9.10). Here,  $b = 0.1$ ,  $d = 0.05$ , and  $N = 100$

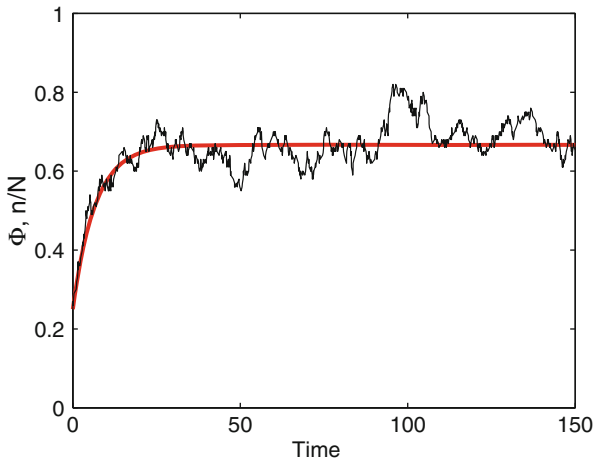
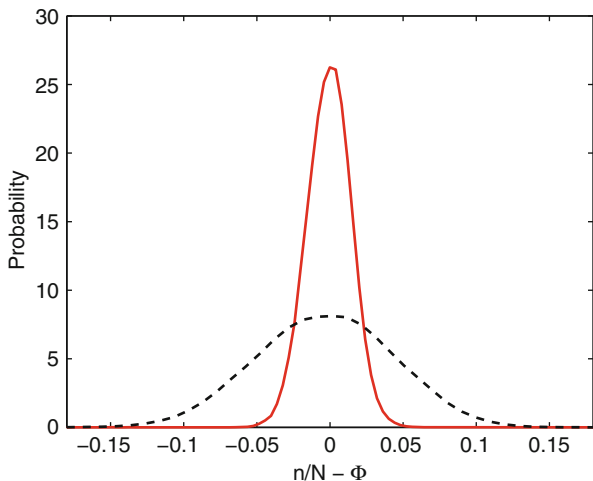


**Fig. 9.2** Normalized histograms of stochastic fluctuations  $n/N - \phi$  recorded from the Gillespie-based simulations. The dashed line refers to  $N = 100$  and the solid line to  $N = 1000$ . The parameters are  $b = 0.1$ ,  $d = 0.05$



The van Kampen ansatz consists in splitting the finite-size concentration  $n/N$  into two contributions. To the continuous (mean-field) concentration  $\phi$ , it is superposed a stochastic term which is supposed to scale as  $1/\sqrt{N}$ . In formulae

$$\frac{n}{N} = \phi + \frac{\xi}{\sqrt{N}} \tag{9.12}$$

where  $\xi$  is a stochastic variable. The quantity  $1/\sqrt{N}$  is small for moderate or large system sizes and hence plays the role of a perturbative parameter in the van Kampen expansion.

Let us start by rewriting Equation (9.4) in the following compact form:

$$\begin{aligned} \frac{dP}{dt} &= (\mathcal{E}^{+1} - 1) T(n - 1|n)P(n, t) \\ &\quad + (\mathcal{E}^{-1} - 1) T(n + 1|n)P(n, t) \end{aligned} \tag{9.13}$$

where the operators  $\mathcal{E}^{\pm 1}$  are defined as

$$\mathcal{E}^{\pm 1} f(n) = f(n \pm 1) \tag{9.14}$$

$f(\cdot)$  being an arbitrary function of the discrete variable  $n$ . The above operators admit a straightforward expansion with respect to  $1/\sqrt{N}$ . A simple manipulation yields in fact to

$$\mathcal{E}^{\pm 1} = 1 \pm \frac{1}{\sqrt{N}} \frac{\partial}{\partial \xi} + \frac{1}{2N} \frac{\partial^2}{\partial \xi^2} + \dots, \tag{9.15}$$

Hence, the first term in the right-hand side of the master equation (9.13) reads

$$\begin{aligned} &(\mathcal{E}^{+1} - 1) T(n - 1|n)P(n, t) \\ &= \left( \frac{1}{\sqrt{N}} \frac{\partial}{\partial \xi} + \frac{1}{2N} \frac{\partial^2}{\partial \xi^2} \right) d \left( \phi + \frac{\xi}{\sqrt{N}} \right) \Pi(\xi, t) \end{aligned} \tag{9.16}$$

where explicit use has been made of the van Kampen ansatz (9.12). By organizing the various terms in the above expressions, one gets:

$$\frac{1}{\sqrt{N}} \left[ d\phi \frac{\partial}{\partial \xi} \Pi \right] + \frac{1}{N} d \left[ \frac{\partial}{\partial \xi} (\xi \Pi) + \frac{1}{2} \phi \frac{\partial^2}{\partial \xi^2} \Pi \right] + \dots \tag{9.17}$$

up to  $1/N$  contributions. Similarly, for the other contribution

$$- \frac{1}{\sqrt{N}} \left[ b(1 - \phi) \frac{\partial}{\partial \xi} \Pi \right] + \frac{1}{N} b \left[ \frac{\partial}{\partial \xi} (\xi \Pi) + \frac{1}{2} (1 - \phi) \frac{\partial^2}{\partial \xi^2} \Pi \right] + \dots \tag{9.18}$$

Using the van Kampen ansatz (9.12) in the left-hand side of the master Eq. (9.13) results in

$$\frac{dP(n, t)}{dt} = \frac{1}{N} \frac{\partial \Pi(\xi, \tau)}{\partial \tau} - \frac{1}{\sqrt{N}} \frac{\partial \Pi(\xi, \tau)}{\partial \xi} \frac{d\phi}{d\tau}. \tag{9.19}$$

where we have set  $P(n, t)$  equal to  $\Pi(\xi, \tau)$  and where  $\tau = t/N$ . Then, one can plug the contributions (9.17–9.19) into the master equation (9.13) and collect together the various terms depending on their respective order in  $1/\sqrt{N}$ . At the leading order, and as expected, we recover the mean-field Eq. (9.10). At the next to leading order instead we obtain the following Fokker–Planck equation [19] for the distribution of fluctuations  $\Pi(\xi, t)$ :



$$\frac{\partial \Pi}{\partial \tau} = (d+b) \frac{\partial}{\partial \xi} (\xi \Pi) + \frac{1}{2} (d\phi + b(1-\phi)) \frac{\partial^2}{\partial \xi^2} \Pi \quad (9.20)$$

The solution of the above one-dimensional Fokker–Planck equation is a Gaussian, whose first and second moments can be readily characterized.

Multiply both sides of the Fokker Planck equation by  $\xi$  and integrate over the real axis in  $d\xi$ . A simple calculation yields to

$$\frac{d\langle \xi \rangle}{d\tau} = -(d+b) \langle \xi \rangle \quad (9.21)$$

where  $\langle \xi \rangle \equiv \int \xi \Pi d\xi$ . The solution of (9.21) is  $\langle \xi \rangle = \langle \xi \rangle_0 \exp[-(d+b)\tau]$ . Asymptotically, when the system settles down to its deputed equilibrium,  $\langle \xi \rangle_{\text{stat}} = \lim_{\tau \rightarrow \infty} \langle \xi \rangle = 0$ .

A similar reasoning applies to the second moment. The latter is defined as  $\langle \xi^2 \rangle \equiv \int \xi^2 \Pi d\xi$  and obeys to the differential equation

$$\frac{d\langle \xi^2 \rangle}{d\tau} = -2(d+b) \langle \xi^2 \rangle + [(d-b)\phi + b] \quad (9.22)$$

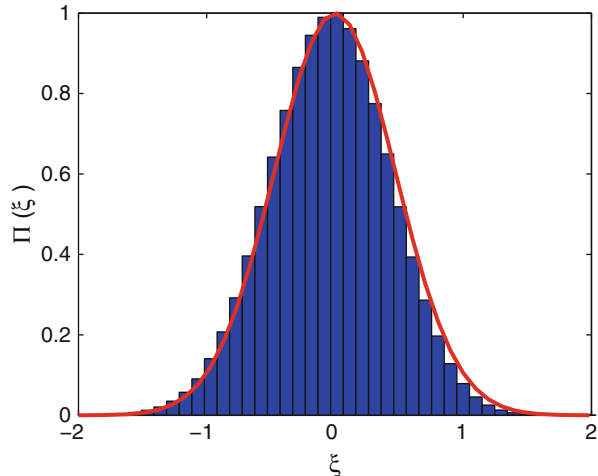
Assume we are interested in the statistics fluctuations around the stationary point when  $\phi \rightarrow \phi^*$ . Clearly, because of stationary,  $d\langle \xi^2 \rangle / d\tau = 0$  in Eq. (9.22) which implies

$$\langle \xi^2 \rangle_{\text{stat}} = \frac{db}{(d+b)^2} \quad (9.23)$$

where use has been made of the expression  $\phi^* = \frac{b}{d+b}$ . The knowledge of the first two moments makes it possible to calculate the stationary (Gaussian) distribution  $\Pi(\xi)$  and draw a direct comparison with the results of the stochastic simulations. This is done in Fig. 9.3: An excellent agreement is found. The van Kampen expansion constitutes therefore a viable strategy to quantify the impact of finite-size corrections that stem from the discrete nature of the simulated medium and beyond the customarily adopted mean-field approximation. Notice that non-Gaussian fluctuations can develop when the system is made to evolve close to an absorbing barrier. Including higher order corrections in the van Kampen expansion, beyond the next-to-leading approximation, allows one to capture the non-Gaussian traits of the distribution [20–22].

In the simple applications that we have here discussed, the stochastic fluctuations materialize in erratic disturbances of the mean-field trajectory. More complex scenarios are however possible. Surprisingly enough, in fact, the microscopic noise that is seeded by finite-size corrections can also yield to macroscopically organized patterns, both in time and space. The van Kampen technique, illustrated above with reference to a simple problem, provides us with an excellent tool to eventually explain such a peculiar behavior. In the following, building on the general ideas presented above, and with reference to a model of biological interest, we shall discuss these intriguing dynamical features. The model that we will discuss has been investigated in [11, 12] and can be seen as a minimal model of a (proto)cell.

**Fig. 9.3** The histogram of rescaled stochastic fluctuations  $\xi$  recorded from the Gillespie-based simulations is compared to the analytical solution of the Fokker-Planck equation (*solid line*). The agreements are excellent and point to adequacy of the van Kampen technique. Here,  $N = 100$ ,  $b = 0.1$ , and  $d = 0.05$



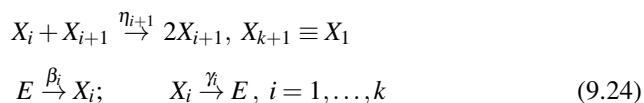
Birth and death reactions, identical to the ones hypothesized above, are still assumed to hold. The model deals however with an arbitrary large number of independent populations, which are organized in a close autocatalytic cycle. These two additional ingredients, dimensions and mutual interactions, will make the dynamics less trivial, in particular as concerns the impact of the endogeneous fluctuations.

## 9.4 A Model of Autocatalytic Reactions

In this section, we will review the application of the system-size expansion to a model of autocatalytic reactions, first introduced in the literature by Togashi and Kaneko [23, 24]. The results that we are going to discuss have been presented in [11, 12]. In the following, we shall start by providing a concise description of the analysis carried out for the aspatial version of the model, which proves less cumbersome from the mathematical viewpoint [11]. Then, we will turn to illustrating the extension to the spatial case, as developed in [12].

In the original scheme devised by Togashi and Kaneko, the reactions are cyclic and involve  $k$  constituents  $X_1, \dots, X_k$ . The latter react according to  $X_i + X_{i+1} \rightarrow 2X_{i+1}$  with  $X_{k+1} \equiv X_1$ ,  $i = 1, \dots, k$ . The chemicals are assumed to be in a container which is well stirred, but with the possibility of diffusing across the surface of the container into a particle reservoir. In [11] the above model has been slightly revisited via explicit inclusion of the null constituents  $E$ .

More specifically, the autocatalytic reaction scheme investigated in [11] reads



where  $r_i$ ,  $\gamma_i$  and  $\beta_i$  (with  $r_{k+1} \equiv r_1$ ) are the rates at which the reactions take place. As explained in the preceding section, the pseudo-chemical elements  $E$  accounts for a finite carrying capacity of the scrutinized system. By denoting the size of the system with  $N$  and labeling  $n_i$  the number of elements of type  $X_i$ , then  $\sum_{i=1}^k n_i + n_E = N$ , where  $n_E$  is the number of empties  $E$ . Clearly, as an obvious consequence of the latter conservation law,  $n_E$  is always replaced by  $N - \sum_{i=1}^k n_i$ . The rate constants  $\gamma_i$  and  $\beta_i$  in Eq. (9.24) control the interactions of the system with the particle reservoir outside the container. In effect  $\gamma_i$  and  $\beta_i$  are the rates at which molecules enter and exit the system in stringent analogy with birth and death rates.

Besides their interest per se, it is speculated that autocatalytic cycles might have been fundamental, back at the origin of life, in sustaining the development of elementary cell-like entities, the so-called protocells. The shared view is that protocell's volume might have been occupied by interacting families of replicators, organized in nested autocatalytic reactions. The latter have been invoked in fact as a possible solution of the famous Eigen's paradox, a simple logic argument that implies limiting the size of self-replicating molecules to perhaps a few hundred base pairs. At odd, almost all life on Earth requires much longer molecules to encode for their genetic information. This problem is handled in living cells by the presence of enzymes which repair mutations, allowing the encoding molecules to reach sizes on the order of millions of base pairs. In primordial organisms, autocatalytic cycles might have provided the necessary degree of microscopic cooperation to prevent the Eigen's drive to self-destruction to eventually take place. In this respect, model (9.24) can constitute a sort of null model of a primordial cell. Hence, the volume where the chemicals are confined can be imagined to be delimited by the cell wall, the membrane.

In the following, we shall report about the study in [11], where the (aspatial) model introduced above has been investigated via the van Kampen perturbative technique. We will in particular show that the discreteness of the constituents that take part to the autocatalytic cycle gives rise to large sustained oscillations, even when the number of elementary units is quite large, and as opposed to mean-field predictions.

## 9.5 The Aspatial Model: Deterministic and Stochastic Dynamics

Let us consider the aspatial version of the autocatalytic cycle, as described by Eq. (9.24). Molecules are supposed to be uniformly stirred inside a given volume. A scalar quantity for each of the  $k$  species is therefore sufficient to unambiguously photograph the state of the system. In other terms, the state of the system is labeled by the  $k$  dimensional vector  $\mathbf{n} \equiv (n_1, \dots, n_k)$ . Under the assumption that the transitions from this state to any other compatible with the former only depend on these integers, the system is Markov and can be described in terms of a master

equation. As illustrated in the preceding sections, the master equation is specified if the transition rates  $T(\mathbf{n}'|\mathbf{n})$  from the state  $\mathbf{n}$  to the state  $\mathbf{n}'$  are given. The assumption of a uniform distribution inside the volume implies that the probability of a reaction taking place is proportional to its rate and the number of reactant molecules. For our case, see Eq. (9.24) the transition rates take the form

$$\begin{aligned} T(n_1, \dots, n_i - 1, n_{i+1} + 1, \dots, n_k | \mathbf{n}) &= \eta_{i+1} \frac{n_i}{N} \frac{n_{i+1}}{N} \\ T(n_1, \dots, n_i + 1, \dots, n_k | \mathbf{n}) &= \beta_i \left( 1 - \frac{\sum_{j=1}^k n_j}{N} \right) \\ T(n_1, \dots, n_i - 1, \dots, n_k | \mathbf{n}) &= \gamma_i \frac{n_i}{N} \end{aligned} \quad (9.25)$$

The master equation for the probability that the system is in state  $\mathbf{n}$  at time  $t$ ,  $P(\mathbf{n}, t)$ , can be hence written as

$$\begin{aligned} \frac{dP(\mathbf{n}, t)}{dt} &= \sum_{i=1}^k (\mathcal{E}_i \mathcal{E}_{i+1}^{-1} - 1) \\ &\times [T(n_1, \dots, n_i - 1, n_{i+1} + 1, \dots, n_k | \mathbf{n}) P(\mathbf{n}, t)] \\ &+ \sum_{i=1}^k (\mathcal{E}_i^{-1} - 1) [T(n_1, \dots, n_i + 1, \dots, n_k | \mathbf{n}) P(\mathbf{n}, t)] \\ &+ \sum_{i=1}^k (\mathcal{E}_i - 1) [T(n_1, \dots, n_i - 1, \dots, n_k | \mathbf{n}) P(\mathbf{n}, t)] \end{aligned} \quad (9.26)$$

where  $\mathcal{E}_i^{\pm 1}$  are a generalization of the step operators previously introduced:

$$\mathcal{E}_i^{\pm 1} f(\mathbf{n}) = f(n_1, \dots, n_i \pm 1, \dots, n_k) \quad (9.27)$$

To progress in the analysis we put forward the aforementioned van Kampen ansatz that, in this case, reads

$$\frac{n_i}{N} = \phi_i(t) + \frac{\xi_i(t)}{\sqrt{N}} \quad (9.28)$$

$\phi_i(t)$  refers to the deterministic contribution. It labels the fraction of the molecules which are of type  $X_i$  at time  $t$  in the mean-field ( $N \rightarrow \infty$ ) limit. The fluctuations  $\xi_i(t)$ , i.e., the stochastic component of the dynamics, are multiplied by the scaling factor  $1/\sqrt{N}$ . Inserting equation (9.28) into Eq. (9.26) allows one to expand the master equation as a power series of  $1/\sqrt{N}$ . By expanding the step operators (9.27) one obtains the usual expressions:

$$\mathcal{E}_i^{\pm 1} = 1 \pm \frac{1}{\sqrt{N}} \frac{\partial}{\partial \xi_i} + \frac{1}{2N} \frac{\partial^2}{\partial \xi_i^2} + \dots \quad (9.29)$$

If we set  $P(\mathbf{n}, t)$  equal to  $\Pi(\xi, \tau)$ , one can expand the left-hand side of the master equation in analogy with what previously done, namely,

$$\frac{dP(\mathbf{n}, t)}{dt} = \frac{1}{N} \frac{\partial \Pi(\xi, \tau)}{\partial \tau} - \frac{1}{\sqrt{N}} \sum_{i=1}^k \frac{\partial \Pi(\xi, \tau)}{\partial \xi_i} \frac{d\phi_i}{d\tau} \quad (9.30)$$

where  $\tau = t/N$ . Substituting Eq. (9.28) into the right-hand side of the master Eq. (9.26) and using the explicit form of the transition rates as reported in (9.25), one may group together the terms of same order in  $1/\sqrt{N}$ .

To leading order, the expanded master equation gives (see [11] for additional information on the algebraic, intermediate steps involved)

$$\frac{d\phi_i}{d\tau} = (\eta_i \phi_{i-1} - \eta_{i+1} \phi_{i+1}) \phi_i + \beta_i \left( 1 - \sum_{j=1}^k \phi_j \right) - \gamma_i \phi_i \quad (9.31)$$

The above equations represent a deterministic approximation to the stochastic model (9.24). Assume  $\eta_i$ ,  $\gamma_i$  and  $\beta_i$  to be the same for each species, and so drop the index  $i$ . The continuous, time-dependent, concentration  $\phi_i$  of species  $i$  evolves starting from the assigned initial condition and asymptotically converges to a (stable) solution  $\phi^*$ , which can be readily obtained by setting  $d\phi_i/d\tau = 0$ . One immediately gets

$$\phi^* = \frac{\beta}{\gamma + k\beta} \quad (9.32)$$

How accurate is the deterministic approximation for the stochastic model here considered? To answer this question one can perform numerical simulations of the chemical reaction system (9.24) by use of the exact Gillespie algorithm [17, 18]. In Fig. 9.4 the outcome of the stochastic simulations (solid line) is compared to the solution of the deterministic equation (9.31) (dashed line). Once the initial transient has died out the latter tends to relax to the deputed equilibrium  $\phi^*$ . At variance, the stochastic time series keeps on oscillating around the reference value  $\phi^*$ . Such regular oscillations, termed quasi-cycles, manifest because of the finite-size corrections to the idealized mean-field dynamics. As we will make clear in the following, the emergence of the quasi-cycles can be successfully explained by retaining the higher order terms in the above perturbative analysis.

At next order of the perturbative development, one finds in fact the following Fokker–Planck equation:

$$\frac{\partial \Pi}{\partial \tau} = - \sum_i \frac{\partial}{\partial \xi_i} [A_i(\xi) \Pi] + \frac{1}{2} \sum_{i,j} B_{ij} \frac{\partial^2 \Pi}{\partial \xi_i \partial \xi_j} \quad (9.33)$$

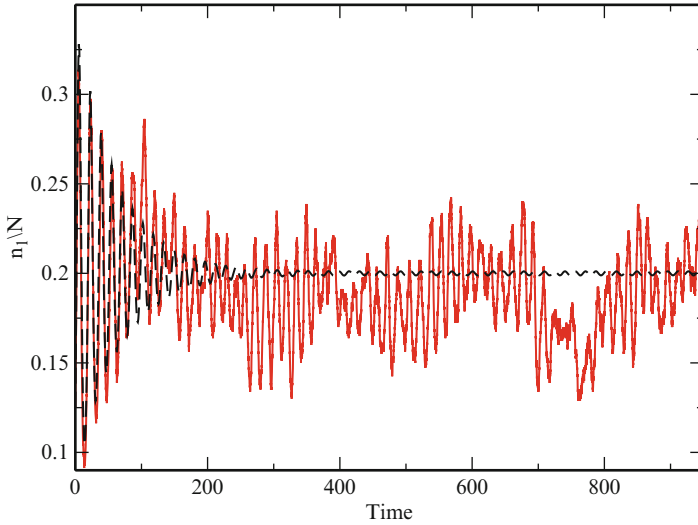


**Fig. 9.4** Temporal evolution of one of the species concentrations for a system composed by  $k = 4$  species and parameters set as  $N = 8190$ ,  $r_i = 10$ , and  $\alpha_i = \beta_i = 1/64 \forall i$ . The noisy line represents one stochastic realization obtained via the Gillespie algorithm [17, 18]. The dashed line shows the numerical solution of the deterministic system given by Eq. (9.31)

which governs the dynamics of the distribution function of fluctuations  $\Pi(\xi, t)$ . Here,

$$\begin{aligned}
 A_i(\xi) = & (\eta_i \phi_{i-1} - \eta_{i+1} \phi_{i+1}) \xi_i + \eta_i \phi_i \xi_{i-1} \\
 & - \eta_{i+1} \phi_i \xi_{i+1} - \beta_i \sum_{j=1}^k \xi_j - \gamma_i \xi_i
 \end{aligned}
 \tag{9.34}$$

and

$$B_{ij} = \begin{cases} -\eta_i \phi_{i-1} \phi_i, & \text{if } j = i - 1 \\ \eta_{i+1} \phi_i \phi_{i+1} + \eta_i \phi_i \phi_{i-1} \\ + \beta_i \left( 1 - \sum_{j=1}^k \phi_j \right) + \gamma_i \phi_i, & \text{if } j = i \\ -\eta_{i+1} \phi_i \phi_{i+1}. & \text{if } j = i + 1 \end{cases}
 \tag{9.35}$$

In Eqs. (9.34) and (9.35),  $\phi_{k+1} \equiv \phi_1$  and  $\xi_{k+1} \equiv \xi_1$ , which follows from the cyclic nature of the model.

Since the  $A_i(\xi)$  are linear functions of the  $\xi_j$  we may write them as

$$A_i(\xi) = \sum_{j=1}^k M_{ij} \xi_j
 \tag{9.36}$$

The probability distribution  $\Pi(\xi, \tau)$  is therefore entirely determined by the two  $k \times k$  matrices  $M$  and  $B$ , whose elements are solely functions of the mean-field concentration  $\phi_j$ . In principle the matrices  $M$  and  $B$  are time dependent, since  $\phi_j$  is. However, in practice we are interested in fluctuations about the stationary state, and so replace  $\phi_j$  with its asymptotic constant analogue  $\phi^*$ .

The Fokker–Planck Eq. (9.33) yields to the equivalent Langevin formulation:

$$\frac{d\xi_i}{d\tau} = \sum_{j=1}^k M_{ij} \xi_j(\tau) + \eta_i(\tau) \tag{9.37}$$

where  $M$  follows from (9.36) and  $\eta_i$  is a Gaussian white noise with zero mean and correlator

$$\langle \eta_i(\tau) \eta_j(\tau') \rangle = B_{ij} \delta(\tau - \tau') \tag{9.38}$$

To bring into evidence the oscillatory nature of the fluctuations, we take the Fourier transform of Eq. (9.37):

$$\sum_{j=1}^k (-i\omega \delta_{ij} - M_{ij}) \tilde{\xi}_j(\omega) = \tilde{\eta}_i(\omega) \tag{9.39}$$

where the  $\tilde{f}$  stands for the Fourier transform of the function  $f$ . Introducing  $\Phi_{ij}(\omega) = -i\omega \delta_{ij} - M_{ij}$  the solution to Eq. (9.39) is

$$\tilde{\xi}_i(\omega) = \sum_{j=1}^k \Phi_{ij}^{-1}(\omega) \tilde{\eta}_j(\omega) \tag{9.40}$$

To identify the dominant frequency of the oscillating time series, one can compute the power spectrum  $P_i(\omega)$  for the  $i$ th species, from Eq. (9.40). In formulae, one gets

$$P_i(\omega) \equiv \langle |\tilde{\xi}_i(\omega)|^2 \rangle = \sum_{j=1}^k \sum_{l=1}^k \Phi_{ij}^{-1}(\omega) B_{jl} (\Phi^\dagger)_{li}^{-1}(\omega) \tag{9.41}$$

In Figs. 9.5 and 9.6, the theoretical power spectra are compared to the homologous quantities calculated from averaging over many realization of the Gillespie-based simulations. The figures refer respectively to  $k = 4$  and  $k = 8$ . One or two peaks are displayed in the power spectra, pointing to the existence of regular oscillatory behaviors in the recorded signals. Ordered temporal oscillations can therefore spontaneously emerge, driven by the stochastic component of the dynamics and as opposed to what predicted within the idealized mean-field scenario.

In the next section we will briefly turn to discussing the generalized spatial model. This setting has been studied in [12] via the van Kampen system-size expansion. We shall hereafter provide a rather compact description of the analysis, without insisting on the technical details of the calculation that can be found in [12].

**Fig. 9.5** Power spectrum of species  $i = 2$  when  $k = 4$ . The analytical curve is shown as a solid line and the simulation (average over 500 independent realizations) as symbols. Here  $r = 10$ ,  $\gamma = \beta = 5/32$ , and  $N = 5,000$ . Reprinted with permission from [11] Copyright (2009) by the American Physical Society

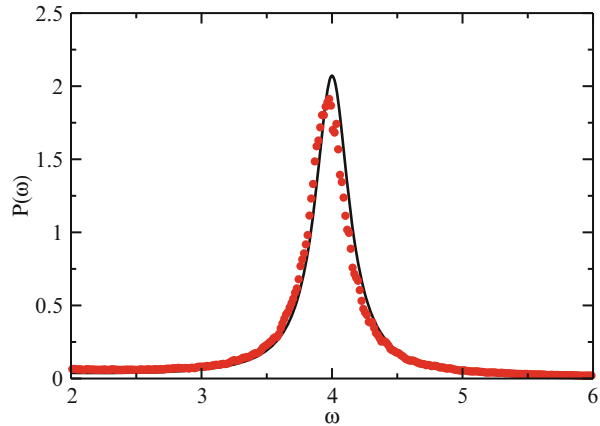
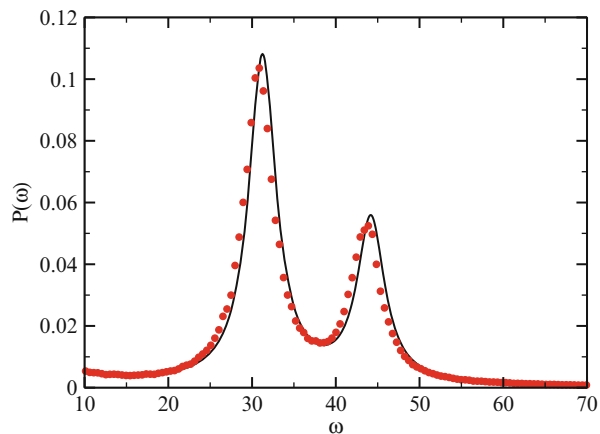


**Fig. 9.6** Power spectrum of the time series for species  $i = 2$  when  $k = 8$ . The analytical result (solid line) is superimposed onto the simulations (symbols), averaged over 500 independent realizations. Here  $r = 200$ ,  $\beta = 1.9$ ,  $\gamma = 2$ , and  $N = 7,000$ . Reprinted with permission from [11], Copyright (2009) by the American Physical Society



### 9.6 Spatial Model: Ordered Patterns Revealed by the van Kampen System Size Expansion

Model (9.24) can be also straightforwardly extended so to explicitly account for the notion of space, as done in [12]. The idea is to coarse-grain the volume where molecules are confined, by partitioning it in  $\Omega$  small micro-cells, within which autocatalytic reactions do occur. Following [12], the  $k$  species are labeled  $X_s^j$ . The index  $s$  identifies the species, while  $j = 1, \dots, \Omega$  refers to the micro-cell to which the element is bound. In analogy with the preceding discussion the reactions can be cast in the form



where  $X_{k+1}^j = X_1^j$ .



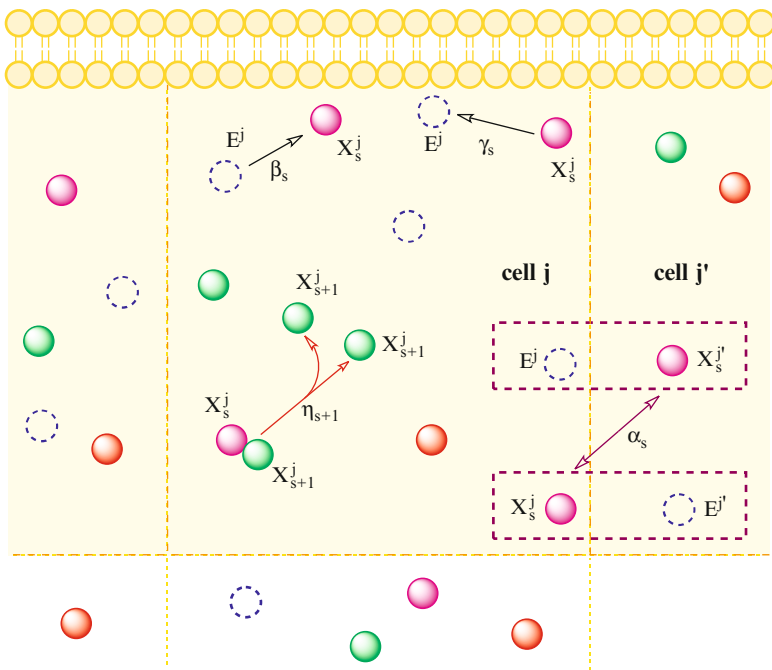


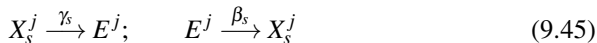
**Fig. 9.7** The volume of the cell is imagined to be partitioned into  $\Omega$  micro-cells. Within micro-cell  $j$  the molecular species interact according to the autocatalytic reactions specified by Eq. (9.24). In addition, the molecules can migrate from micro-cell  $j$  to its nearest neighbors, e.g., micro-cell  $j'$ , as depicted in the cartoon. A molecule of type  $X_k^j$  (full circle) takes over a vacancy (dashed empty circle) of micro-cell  $E^{j'}$  and so transforms into  $X_k^{j'}$ , leaving behind a vacancy  $E^j$ . Finally, the chemical can also diffuse in from the environment, a reaction that in turn implies changing  $E^j$  into  $X_k^j$ . The opposite holds for molecules that diffuse out into the environment. Reprinted with permission from [12], Copyright (2010) by the American Physical Society

Indeed, only the region that is adjacent to the outer boundary, the cell membrane as emphasized above, is given a detailed spatial structure. The remaining inner volume acts instead as a particle reservoir. A cartoon of the setting here imagined is depicted in Fig. 9.7. Molecules sitting in cell  $j$  can migrate towards the neighbors micro-cell  $j'$ . This is a microscopic process that obeys to the following chemical equations:



where  $E^j$  (resp.  $E^{j'}$ ) represents vacancies in cell  $j$  (resp.  $j'$ ). The capacity of each micro-cell is  $N$ : the sum of the number of molecules of each species plus the number of vacancies equals  $N$ , for every micro-cell.

Finally, a molecule  $X_s^j$  can migrate from cell  $j$  towards the (outer) environment or the inner region leaving behind an empty case  $E^j$ . Alternatively, cell  $j$  can gain a molecule  $X_s^j$  from the environment or inner region. These processes are described as



When operating in this generalized setting, the mathematical analysis becomes more complex, as compared to the aspatial model. One additional index has to be forcefully introduced in the definition of the variables involved so to specify the micro-cell to which the molecules belong. In other words, the discrete concentration  $n_s^j$  is not just function of time but also sensitive to the specific spatial location. This additional degree of freedom will make it possible to eventually appreciate the emergence of spatially organized patterns. The state of the system can be characterized by the vector  $\mathbf{n} = (\mathbf{n}^1, \mathbf{n}^2, \dots, \mathbf{n}^\Omega)$  where  $\mathbf{n}^j = (n_1^j, n_2^j, \dots, n_k^j)$ .

The model can be formulated in terms of a chemical master equation. Then, by applying the van Kampen perturbative scheme, one can recover the mean-field solution and determine as well the stochastic, finite  $N$ , corrections to it. The transition rates associated to the migration from one cell to the neighbor one read

$$\begin{aligned} T(n_s^j - 1, n_s^{j'} + 1 | n_s^j, n_k^{j'}) &= \frac{\alpha_s}{z\Omega} \frac{n_s^j}{N} \left( 1 - \sum_{m=1}^k \frac{n_m^{j'}}{N} \right) \\ T(n_s^j + 1, n_s^{j'} - 1 | n_s^j, n_k^{j'}) &= \frac{\alpha_s}{z\Omega} \frac{n_s^{j'}}{N} \left( 1 - \sum_{m=1}^k \frac{n_m^j}{N} \right) \end{aligned} \quad (9.46)$$

where  $z$  is the number of nearest neighbors that each micro-cell has. The reaction rates associated to the autocatalytic cycles and to the diffusion from/to the inner/outer bulk can be written as a trivial extension of the equivalent quantities obtained for the aspatial model. For this reason, these are not given here explicitly.

The master equation for the probability  $P(\mathbf{n}, t)$  can be cast in the form

$$\begin{aligned} \frac{dP(\mathbf{n}, t)}{dt} &= \sum_{j=1}^{\Omega} \mathcal{T}_{\text{loc}}^j P(\mathbf{n}, t) + \sum_{j=1}^{\Omega} \sum_{j' \in j} \mathcal{T}_{\text{mig}}^{jj'} P(\mathbf{n}, t) \\ &+ \sum_{j=1}^{\Omega} \mathcal{T}_{\text{env}}^j P(\mathbf{n}, t), \end{aligned} \quad (9.47)$$

where the three terms on the right-hand side refer respectively to the local chemical reactions, the migration of species between micro-cells, and the interaction with the outer/inner environment. The notation  $j' \in j$  indicates that cell  $j'$  is a nearest neighbor of the cell  $j$ .

The van Kampen analysis requires introducing the ansatz

$$\frac{n_s^j}{N} = \phi_s^j + \frac{1}{\sqrt{N}} \xi_s^j \quad (9.48)$$

into the master equation and carrying out the perturbative analysis, by adopting  $1/\sqrt{N}$  as a small parameter. The details of the calculations are given in [12] and we shall here solely summarize the results for what concerns the leading and next-to-leading approximations.

At the leading order, one finds the following equation for the concentration  $\phi_s^j$  of species  $s$  in cell  $j$ :

$$\begin{aligned} \frac{d\phi_s^j}{d\tau} &= \eta_s \phi_{s-1}^j \phi_s^j - \eta_{s+1} \phi_s^j \phi_{s+1}^j \\ &+ \alpha_s \left( \Delta \phi_s^j \left( 1 - \sum_{m=1}^k \phi_m^j \right) + \phi_s^j \sum_{m=1}^k \Delta \phi_m^j \right) \\ &+ \beta_s \left( 1 - \sum_{m=1}^k \phi_m^j \right) - \gamma_s \phi_s^j \end{aligned} \quad (9.49)$$

where  $\Delta$  stands for the discrete Laplacian operator  $\Delta f_s^j = (2/z) \sum_{j' \in j} (f_s^{j'} - f_s^j)$ . In the limit where the size of the micro-cells tends to zero, the above equations become partial differential equations,  $\Delta$  converging to the more familiar Laplacian operator. Notice that Eq. (9.49) constitutes the natural generalization of Eq. (9.31) to the case where space is accounted for. Notice the cross-diffusion terms that reflect the assumption of a finite carrying capacity in each micro-cell. The importance of such additional contributions, which follows from a rigorous description of the microscopic diffusion, has been elaborated on in [25]. Assuming  $\eta_s$ ,  $\beta_s$  and  $\gamma_s$  to be identical for all species, we can drop the index  $s$  and obtain an explicit expression for the homogeneous (uniform in space) fixed point of the dynamics, namely  $\phi^* = \beta/(\gamma + k\beta)$ . As expected, the latter coincides with the fixed point obtained for the aspatial model.

The next-to-leading corrections yield as usual to a Fokker–Planck equation for the distribution of fluctuations (see Eq. B1 in [12]). The Fokker–Planck is formally equivalent to a Langevin equation, which upon spatial Fourier reads

$$\frac{d\xi_s^{\mathbf{k}}}{d\tau} = \sum_r M_{sr}^{\mathbf{k}} \xi_r^{\mathbf{k}} + \lambda_s^{\mathbf{k}}(\tau) \quad (9.50)$$

where

$$\langle \lambda_s^{\mathbf{k}}(\tau) \lambda_r^{\mathbf{k}'}(\tau') \rangle = \mathcal{B}_{sr}^{\mathbf{k}} \Omega a^d \delta_{\mathbf{k}+\mathbf{k}',0} \delta(\tau - \tau') \quad (9.51)$$

and where  $\mathbf{k}$  is the wavevector. To derive the above result it was assumed in [12] that the micro-cells form a hypercubic lattice in  $d$ -dimensions with linear spacing  $a$ . The matrix  $M^{\mathbf{k}}$  is

$$M_{sr}^{\mathbf{k}} = M_{sr}^{(\text{NS})} + M_{sr}^{(\text{SP})} \Delta_{\mathbf{k}} \quad (9.52)$$

where  $\Delta_{\mathbf{k}}$  is the Fourier transform of the discrete Laplacian

$$\Delta_{\mathbf{k}} = \frac{2}{d} \sum_{\gamma=1}^d [\cos(\mathbf{k}_{\gamma} a) - 1] \quad (9.53)$$

and  $k_{\gamma}$  is one of  $\gamma$ th component of the vector  $\mathbf{k}$ . The two matrices  $M^{(\text{NS})}$  and  $M^{(\text{SP})}$  are

$$M_{ss}^{(\text{NS})} = -\beta - \gamma \quad (9.54)$$

$$M_{sr}^{(\text{NS})} = \begin{cases} -\eta \phi^* - \beta, & \text{if } r = s + 1 \\ \eta \phi^* - \beta, & \text{if } r = s - 1 \\ -\beta, & \text{if } |s - r| > 1 \end{cases} \quad (9.55)$$

and

$$M_{ss}^{(\text{SP})} = \alpha_s [1 + (1 - k) \phi^*] \quad (9.56)$$

$$M_{sr}^{(\text{SP})} = \alpha_s \phi^* \text{ if } s \neq r \quad (9.57)$$

NS stands for “non spatial,” while SP is the compact label for “spatial.” The matrix  $\mathcal{B}^{\mathbf{k}}$  in Eq. (9.51) is given by

$$\mathcal{B}_{sr}^{\mathbf{k}} = \mathcal{B}_{sr}^{(\text{NS})} + \mathcal{B}_{sr}^{(\text{SP})} \Delta_{\mathbf{k}} \quad (9.58)$$

where the two  $k \times k$  matrices  $\mathcal{B}^{(\text{NS})}$  and  $\mathcal{B}^{(\text{SP})}$  are given by

$$\mathcal{B}_{ss}^{(\text{NS})} = a^d [\beta(1 - k\phi^*) + \gamma\phi^* + 2\eta(\phi^*)^2] \quad (9.59)$$

$$\mathcal{B}_{sr}^{(\text{NS})} = \begin{cases} -a^d \eta (\phi^*)^2, & \text{if } r = s + 1 \\ -a^d \eta (\phi^*)^2, & \text{if } r = s - 1 \\ 0, & \text{if } |s - r| > 1 \end{cases} \quad (9.60)$$

and

$$\mathcal{B}_{ss}^{(\text{SP})} = -2a^d \alpha_s \phi^* (1 - k\phi^*) \quad (9.61)$$

$$\mathcal{B}_{sr}^{(\text{SP})} = 0 \text{ if } s \neq r \quad (9.62)$$

As discussed above, fluctuations about the stationary state need to be taken into account, as they can be relevant even if  $N$  is relatively large. Since the model extends in space, the power spectrum of fluctuations should depend on both the spatial wavenumber  $\mathbf{k}$  and the frequency  $\omega$ . Defining  $\Phi_{\text{sr}}^{\mathbf{k}}(\omega) = (-i\omega\delta_{\text{sr}} - M_{\text{sr}}^{\mathbf{k}})$ , one eventually obtains [12] the following compact expression for the power spectrum  $P_s(\mathbf{k}, \omega)$  of the fluctuations of species  $s$ :

$$\begin{aligned} P_s(\mathbf{k}, \omega) &\equiv \langle |\xi_s^{\mathbf{k}}(\omega)|^2 \rangle \\ &= \Omega a^d \sum_{r=1}^k \sum_{u=1}^k [\Phi_{\text{sr}}^{\mathbf{k}}(\omega)]_{\text{sr}}^{-1} \mathcal{B}_{\text{ru}}^{\mathbf{k}} [\Phi_{\text{us}}^{\mathbf{k}\dagger}(\omega)]_{\text{us}}^{-1} \end{aligned} \quad (9.63)$$

The analysis sketched above is a straightforward, though complex, generalization of the study of [11] reviewed in the preceding section. We shall be here just concerned with presenting the main conclusion of the analysis, comparing in particular the theoretical power spectra to the homologous quantities obtained via numerical simulations. The analysis is limited to the choice  $d = 1$ , i.e., a one-dimensional frontier (membrane) of a two-dimensional compact domain (cell).

As reported in Fig. 9.8, a localized peak is predicted by the theory. This evidence suggests that organized spatiotemporal patterns can spontaneously emerge, as mediated by the endogenous stochasticity of the system. The plots in Fig. 9.8 refer to two distinct species and are obtained by operating in the setting with  $k = 4$ . The other two species display a similar degree of spatiotemporal self-organization.

The theory prediction, and thus the accuracy of the approximations involved, can be tested via direct simulations. By averaging over many independent realizations, one can calculate the power spectra of the recorded stochastic time series after Fourier transformation. The numerical power spectra are depicted in Fig. 9.9 for the same choice of parameters as in Fig. 9.8. The correspondence between the profiles is remarkably good. Spatial, as well as temporal, order can spontaneously develop as a collective amplification of the microscopic finite-size fluctuations.

## 9.7 Conclusion

Modeling the dynamical evolution of a large sea of mutually interacting entities is a task of great importance and cross-disciplinary interest. The customarily adopted scenario assumes dealing with continuous populations, whose concentrations change in space and time according to the governing partial or ordinary differential equations. In doing so, one neglects the intimate discreteness of the investigated medium to favor a mean-field deterministic approach. In many cases, however, the finite-size fluctuations stemming from the microscopic graininess, and therefore endogenous to the system under scrutiny, prove crucial. They can in fact amplify as follows a complex resonance mechanism and yield to organized spatiotemporal patterns. More specifically, the measured concentrations which re-

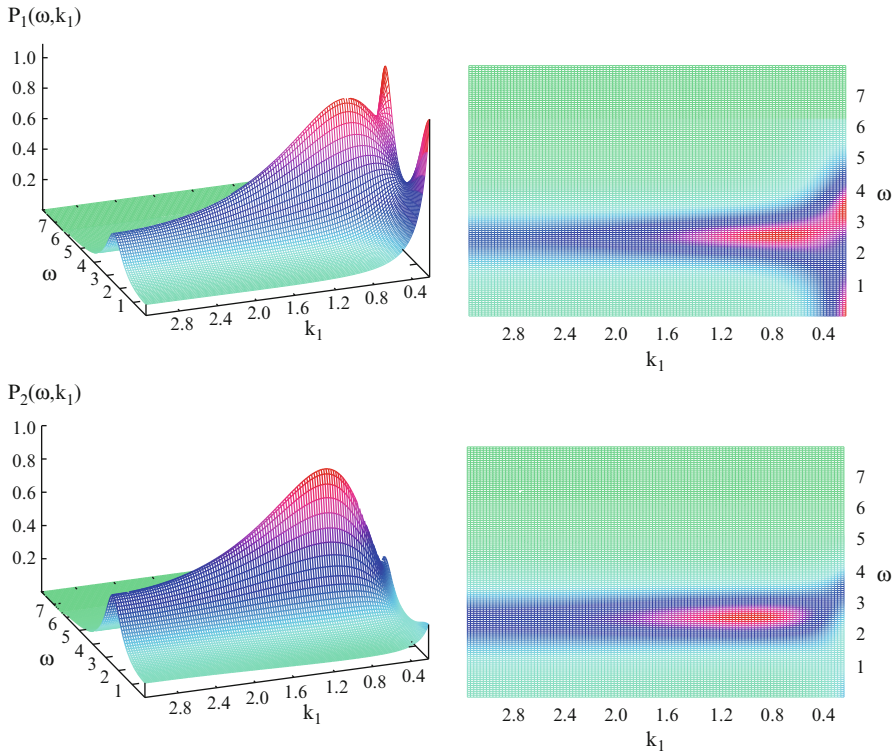


**Fig. 9.8** Analytical power spectra calculated via the van Kampen system-size expansion; see [12] for details. The theoretical profiles refer to the case with  $k = 4$  species and to a two-dimensional volume (one-dimensional periodic array of  $\Omega$  micro-cells). Each three-dimensional plot (and its corresponding two-dimensional projection) refers to a different chemical species. A localized peak is shown, which implies the existence of regular spatiotemporal patterns. Here  $\Omega = 256$ ,  $\eta = 10$ ,  $\beta = 5/32$ ,  $\gamma = 5/32$ , and  $\alpha = [100, 0.001, 1, 500]$ . Reprinted from [12]

flect the distribution of the interacting entities (e.g., chemical species, biomolecules) can oscillate regularly in time and/or display spatially patched profiles, collective phenomena which testify on a surprising degree of macroscopic order, as mediated by the stochastic component of the dynamics.

These intriguing phenomena have been recently addressed and successfully explained via rigorous analytical means. Among other techniques, the van Kampen system-size expansion can be employed to bridge the gap between the deterministic and stochastic viewpoints. In this chapter, we have provided a pedagogical introduction to such method, by considering a simple birth and death stochastic process, which accounts for the finite carrying capacity of the embedding volume. The theoretical calculations enabled us to quantify the probability distribution function of fluctuations around the stationary fixed point. The adequacy of the prediction was confirmed by direct comparison with the outcome of stochastic

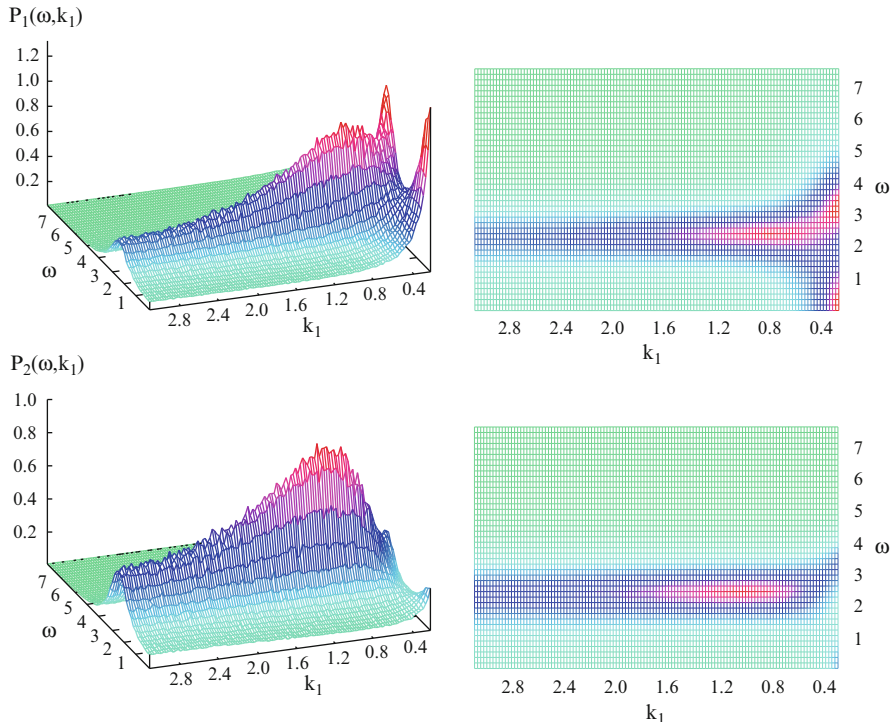


**Fig. 9.9** Numerically calculated power spectra are obtained from averaging 800 realizations; see [12] for further information. Stochastic simulations are performed via the Gillespie algorithm. Parameters are set to the same values assigned when drawing the theoretical plots of Fig. 9.8. Here  $N = 5,000$ . Reprinted from [12]

simulations. In this case the fluctuations result in random, Gaussian-distributed disturbances around the stable fixed point of the dynamics.

More interestingly, it is the application of the van Kampen system-size expansion to a stochastic model of autocatalytic reactions. The model, introduced by Togashi and Kaneko [23] and later on revisited by Di Patti and collaborators [11], is presumably relevant for studies on the origin of life and exists into two versions, respectively: the aspatial [11] and spatial one [12]. By operating in these contexts and making use of the system-size expansion, one can show that the chemical constituents can organize in regular spatiotemporal cycles, coherent macroscopic structures that emerge from the microscopic disorder. In both cases, the perturbative scheme pioneered by van Kampen turns out to be accurate and versatile. It thus represents a powerful and reliable tool to inspect the role played by demographic fluctuations in a finite-size population, beyond the idealized mean-field approximation.

**Acknowledgements** A large portion of this paper is devoted to reviewing the results of [11, 12] which I coauthored with my colleagues T. Dauxois, P. De Anna, F. Di Patti, and A. McKane. I wish to thank them all.

## References

1. J.D. Murray, *Mathematical Biology*, 2nd edn. (Springer, Heidelberg, Germany, 1993)
2. B. Alberts et al., *Molecular Biology of the Cell*, 5th edn. (Garland Science, New York, 2007)
3. H. Lodish et al., *Molecular Cell Biology*, 6th edn. (W.H. Freeman and Co., New York, 2008)
4. J. Maynard Smith, *Models in Ecology* (Cambridge University Press, Cambridge, 1974)
5. C.W. Gardiner, *Handbook of Stochastic Methods*, 3rd edn. (Springer-Verlag, Berlin, 2004)
6. N.G. van Kampen, *Stochastic Processes in Physics and Chemistry*, 3rd edn. (Elsevier, Amsterdam, 2007)
7. A.J. McKane, T.J. Newman, Phys. Rev. Lett. **94**, 218102 (2005)
8. A.J. McKane, J.D. Nagy, T.J. Newman, M.O. Stefanini, J. Stat. Phys. **128**, 165 (2007)
9. D. Alonso, A.J. McKane, M. Pascual, J. R. Soc. Interface **4**, 575 (2007)
10. A.J. McKane T.J. Newman, Phys. Rev. E **70**, 041902 (2004)
11. T. Dauxois, F. Di Patti, D. Fanelli, A.J. McKane, Phys. Rev. E **79**, 036112 (2009)
12. P. De Anna, F. Di Patti, D. Fanelli, A.J. McKane, T. Dauxois, Phys. Rev. E **81** 81 056110 (2010)
13. T. Biancalani, D. Fanelli, F. Di Patti, Phys. Rev. E **81**, ISSN: 1539–3755 (2010)
14. S. Strogatz, *Non Linear Dynamics and Chaos: With Applications to Physics, Biology, Chemistry and Engineering* (Perseus Book Group, Cambridge, MA, 2001)
15. M.S. Bartlett, J. R. Stat. Soc. A **120**, 48 (1957)
16. R.M. Nisbet, W.S.C. Gurney, *Modelling Fluctuating Populations* (Wiley, New York, 1982)
17. D.T. Gillespie, J. Comput. Phys. **22**, 403 (1976)
18. D.T. Gillespie, J. Phys. Chem. **81**, 2340 (1977)
19. H. Risken, *The Fokker–Planck Equation*, 2nd edn. (Springer-Verlag, Berlin, 1989)
20. C. Cianci, F. Di Patti, D. Fanelli, Europ. Phys. Lett. **96**, 50011 (2011)
21. C. Cianci, F. Di Patti, D. Fanelli, L. Barletti, preprint arXiv:1104.5668 (2011)
22. Grima R., Phys. Rev. Lett. **102**, 218103 (2009)
23. Y. Togashi, K. Kaneko, Phys. Rev. Lett. **86**, 2459 (2001)
24. Y. Togashi, K. Kaneko, J. Phys. Soc. Jpn. **72**, 62 (2003)
25. D. Fanelli, A. McKane, Phys. Rev. E **82**, 021113 (2010)